

## Research Article

# Study on Ring-Opening Copolymerization of Trioxymethylene and Second Monomer Initiated by Phosphotungstic Acid

Yanhong Li <sup>1</sup>, Yushun Jin <sup>1</sup>, Hongjuan Li,<sup>2</sup> Xiang Li,<sup>2</sup> Yatao Wang,<sup>2</sup> Ruofan Liu,<sup>1</sup> and Yibo Wu <sup>1</sup>

<sup>1</sup>Beijing Institute of Petrochemical Technology, Beijing 102617, China

<sup>2</sup>Kailuan (Group) Co., Ltd., Tangshan, Hebei 063018, China

Correspondence should be addressed to Yushun Jin; [jinyushun@bipt.edu.cn](mailto:jinyushun@bipt.edu.cn) and Yibo Wu; [wuyibo@bipt.edu.cn](mailto:wuyibo@bipt.edu.cn)

Received 20 May 2022; Revised 30 July 2022; Accepted 2 August 2022; Published 1 September 2022

Academic Editor: Xin Hu

Copyright © 2022 Yanhong Li et al. This is an open access article distributed under the Creative Commons Attribution License, which permits unrestricted use, distribution, and reproduction in any medium, provided the original work is properly cited.

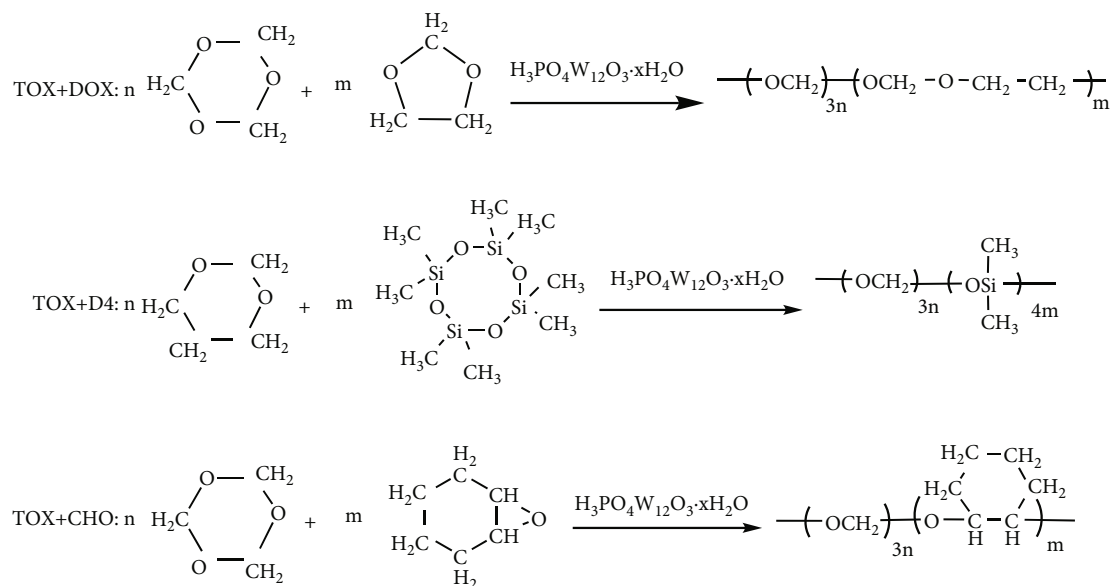
In this study, a series of polyoxymethylene copolymers are synthesized by bulk cationic ring-opening polymerization by 1,3,5-trioxane (TOX) with 1,3-dioxolane (DOX), octamethylcyclotetrasiloxane (D4), and cyclohexane oxide (CHO) as the second monomer using phosphotungstic acid (PTA) as an initiator. The polymer products were characterized by hydrogen nuclear magnetic resonance (<sup>1</sup>H-NMR), infrared spectroscopy (IR), thermogravimetry (TG), and differential scanning calorimetry (DSC). And the copolymerization energy barrier was calculated at the b3lyp/6-31g(d) calculation level using density functional theory (DFT) to explore the copolymerization ability of the second monomer with 1,3,5-trioxane. The results showed that CHO as the second monomer more easily participated in the copolymerization reaction, and the copolymers showed better thermal stability.

## 1. Introduction

1,3,5-trioxane (TOX) can be synthesized into high molecular weight, high density, and high crystallinity polyoxymethylene (POM) with -CH<sub>2</sub>O- repeat unit structure through cationic polymerization [1, 2]. Because of its high stiffness and hardness, excellent mechanical properties, good fatigue resistance, and wear resistance, POM can partially replace copper, aluminum, zinc, or other metal materials in various fields such as electrical and electronic industry, machinery industry, and military industry [3, 4]. Therefore, POM is also called “metal plastic” [5]. However, the unstable semiacetal structure (-OCH<sub>2</sub>OH) at the chain end of the polyoxymethylene molecule is easy to degrade under the conditions of light, heat, and oxygen. This shortage has seriously limited POM service performance [6–8]. Therefore, it is necessary to improve the stability of polyoxymethylene for its further development [9–15].

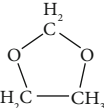
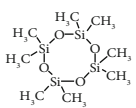
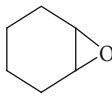
Typically, there are two effective ways to improve the thermal stability of POM, which are the development of an efficient and appropriate initiation system, and the introduc-

tion of new comonomers to change the molecular structure of polyoxymethylene [16–22]. At present, the initiators for copolyformaldehyde are mainly divided into three categories: Lewis acid initiators, protonic acid initiators, and heteropolyacid initiators [12, 23, 24]. Protic acids, such as HClO<sub>4</sub> [25], initiation system has a very fast initiation rate, resulting in a too-short induction period to analyze its properties. The reaction is also too fast, leading to a large instantaneous heat release, which becomes a huge challenge for industrialization. In comparison to proton acid, Lewis acid-boron trifluoride complex [23, 26] (such as BF<sub>3</sub>·O(Bu)<sub>2</sub>, BF<sub>3</sub>·O(Et)<sub>2</sub>) initiation system has moderate reaction temperature, reasonable reaction rate, and the reaction heat can be effectively removed during continuous production, which can ensure the stability of polymerization quality. Thus, the Lewis acid-boron trifluoride complex is the major initiation system used in industry nowadays. However, the polymerization conversion rate depends on the dosage of Lewis acid-boron trifluoride complex initiator usage. If the dosage is too low, the synthesized polymer would be too soft to be dried. Thus, the so-called “wet material”



SCHEME 1: Copolymerization of TOX with the second monomer.

TABLE 1: <sup>1</sup>H-NMR results of copolymerization of TOX with the second monomer.

Serial number	Sample	Second monomer	$n_{(T)}:n_{(O)}(O)^a$ (mol%)	$n_{(T)}:n_{(O)}(O)^b$ (mol%)
	p (TOX-co-DOX)			
1	p (TOX <sub>98</sub> -co-DOX <sub>2</sub> )		98:2 (2%)	99.18:0.52 (0.33%)
2	p (TOX <sub>96</sub> -co-DOX <sub>4</sub> )		96:4(4%)	98.40:1.60(1.60%)
3	p (TOX <sub>94</sub> -co-DOX <sub>6</sub> )		94:6(6%)	96.24:3.76(2.37%)
4	p (TOX <sub>92</sub> -co-DOX <sub>8</sub> )		92:8(8%)	96.10:3.90(3.90%)
5	p (TOX <sub>90</sub> -co-DOX <sub>10</sub> )		90:10(10%)	95.68:4.32(4.32%)
	p (TOX-co-D4)			
6	p (TOX <sub>98</sub> -co-D4 <sub>2</sub> )		98:2(2%)	99.84:0.16(0.16%)
7	p (TOX <sub>96</sub> -co-D4 <sub>4</sub> )		96:4(4%)	99.69:0.31(0.31%)
8	p (TOX <sub>92</sub> -co-D4 <sub>8</sub> )		92:8(8%)	99.66:0.34(0.34%)
9	p (TOX <sub>90</sub> -co-D4 <sub>10</sub> )		90:10(10%)	99.58:0.42(0.42%)
10	p (TOX <sub>88</sub> -co-D4 <sub>12</sub> )		88:12(12%)	99.36:0.64(0.64%)
	p (TOX-co-CHO)			
11	p (TOX <sub>99</sub> -co-CHO <sub>1</sub> )		99:1(1%)	99.76:0.24(0.44%)
12	p (TOX <sub>98</sub> -co-CHO <sub>2</sub> )		98:2(2%)	99.47:0.53(0.60%)
13	p (TOX <sub>97</sub> -co-CHO <sub>3</sub> )		97:3(3%)	98.93:1.07(1.43%)
14	p (TOX <sub>96</sub> -co-CHO <sub>4</sub> )		96:4(4%)	98.51:1.49(2.14%)
15	p (TOX <sub>95</sub> -co-CHO <sub>5</sub> )		95:5(5%)	96.39:3.61(3.24%)

$n_{(T)}:n_{(O)}$  represents the mole ratio of TOX with the second monomer.  $(O)^a$  represents the feeding mole fraction of the second monomer;  $(O)^b$  represents the mole fraction of the second copolymerization component in the total copolymerization component calculated by equations (1)–(3).

phenomenon would appear. Also, the after-treatment of the catalyst is a problem. The residue catalyst is hard to remove from the material. It would finally lead to the decomposition of POM. In comparison, the boron trifluoride initiating system and the heteropolyacid initiating system [27, 28] can initiate polymerization at a smaller dosage. Thereby using this system benefits the posttreatment process. What is more, the heteropolyacid initiation system has a higher reaction rate, and the thermal stability and the conversion

rate of the copolymer can be improved. Thus, heteropolyacid initiation system is a potential system for industrial use to increase the stability of POM.

To provide a new path to improve the thermal stability of POM, in this paper, phosphotungstic acid was used as an initiator to explore the copolymerization of TOX with three epoxy-based second monomers: 1,3-dioxolane (DOX), octamethylcyclotetrasiloxane (D4), and cyclohexane oxide (CHO). The three epoxy-based second monomers are

TABLE 2: Cationic copolymerization of TOX and DOX.

Initiator	Dosage of initiator (ppm)	Yield (%)	$M_n \times 10^4$ (g/mol)	Mw/Mn
$\text{BF}_3 \cdot \text{O}(\text{Bu})_2$	70	75.8	6.9	2.42
$\text{BF}_3 \cdot \text{O}(\text{Bu})_2$	60	75.6	7.2	2.42
$\text{BF}_3 \cdot \text{O}(\text{Bu})_2$	50	76.2	7.6	2.37
$\text{BF}_3 \cdot \text{O}(\text{Bu})_2$	40	58.9	8.4	2.22
$\text{BF}_3 \cdot \text{O}(\text{Bu})_2$	20	—	Nonpolymerization	—
$\text{H}_3\text{PW}_{12}\text{O}_{40}$	12	77.8	8.8	2.36
$\text{H}_3\text{PW}_{12}\text{O}_{40}$	10	78.6	9.8	2.22
$\text{H}_3\text{PW}_{12}\text{O}_{40}$	8	74.3	10.6	2.31
$\text{H}_3\text{PW}_{12}\text{O}_{40}$	6	69.2	13.2	2.12
$\text{H}_3\text{PW}_{12}\text{O}_{40}$	4	—	Nonpolymerization	—

The polymerization temperature is 80 °C. The feeding ratio (mol%) of TOX and DOX is 96 : 4.

available for cationic ring-opening polymerization. Formaldehyde copolymerization would interrupt the carbon and oxygen alternately arranged chain structure of polyoxymethylene. Thus, the amount of the unstable hemiacetal structure at the chain end is reduced. The thermal stability of polyoxymethylene can be improved.

## 2. Experimental

**2.1. Materials.** 1,3,5-trioxane (TOX) was provided by Tangshan Kailuan Group Co., Ltd.; phosphotungstic acid (PTA) and  $\text{BF}_3 \cdot \text{O}(\text{Bu})_2$  are purchased from Sinopharm Group Co., Ltd.; triphenylphosphine (99%) was purchased from J&K Scientific; Calcium stearate (98%) was purchased from Guang Fu Tech. Development Co., Ltd. Melamine (99%) was purchased from Sun Chemical Technology Co., Ltd. N, N'-Ethylenebis (ceramide) (EBS), and Antioxidant 245 were provided by Tangshan Kailuan Group Co., Ltd. These materials were used directly in the experiments without any further treatment. 1,3-dioxolane (DOX, 99.99%), octamethylcyclotetrasiloxane (D4, 98%), and cyclohexane oxide (CHO, 98%) were purchased from J&K Scientific and were purified before use.

**2.2. Acetal Copolymer Synthesis.** In this research, the bulk copolymerization method was used to prepare the POM copolymers. A series of the second monomers synthesized with TOX is shown below in Scheme 1. To synthesize the copolymer, first, the polymerization bottle was vacuumed and filled with nitrogen three times before use. Then, 100 g molten TOX and a certain amount of the second monomer were added to a polymerization bottle and mixed for 15 min at an 80 °C oil bath. The dosages of the second monomers are listed in Table 1. A certain amount of phosphotungstic acid initiator (10 ppm) was then added to the system. The reaction continues from several minutes to hours, depending on the choice of the second monomer. For all reactions, it can be observed that the mixed liquid gradually became cloudy, followed by white solid polymer formed and precipitated at the bottom.

**2.3. Postprocessing of Crude Products.** The residual catalyst will cause the decomposition of the copolymer. It is one of

TABLE 3: Cationic copolymerization of TOX and the second monomer.

Second monomer	Feeding (mol%)	Copolymer (mol%)
DOX	2	0.33
D4	2	0.16
CHO	2	0.60
DOX	4	1.60
D4	4	0.31
CHO	4	2.14

The polymerization temperature is 80 °C.

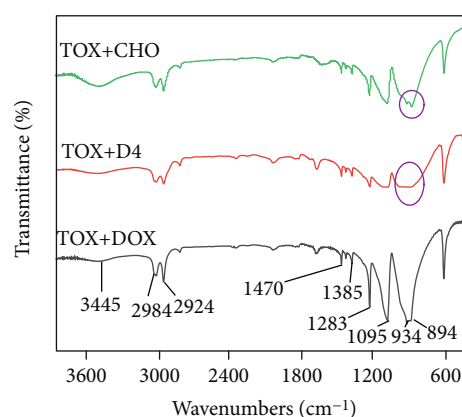


FIGURE 1: IR spectra of the copolymer.

the main reasons decline in the thermal stability of POM. To remove residual initiators, monomers, and the hemiacetal structure which leads to the poor thermal stability of formaldehyde polymers in the polymerization system, post-treatment must be carried out. After the polymerization, the crude product would be mixed with a certain amount of pulverizes, which includes triphenylphosphine, antioxidant 245, calcium stearate, EBS, and melamine. Then, the compound is extruded by a small extruder at 190 °C. The compounds should be kept in the extrusion capillary for 3-5 minutes to ensure powders are fully molten. Then, purified POM was taken to run other characterizations.

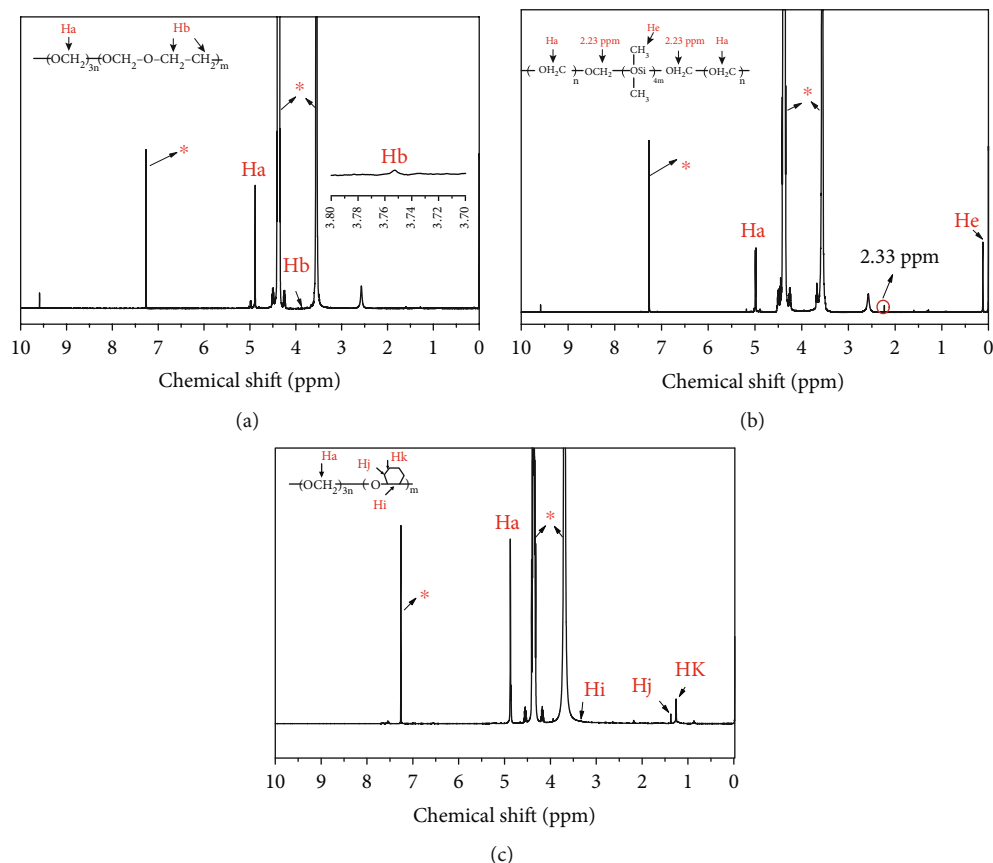


FIGURE 2:  $^1\text{H-NMR}$  spectra of the copolymer. (a) The copolymer of TOX with DOX. (b) The copolymer of TOX with D4. (c) The copolymer of TOX with CHO. Signal \* represents 1,1,1,3,3,3-hexafluoro-2-propanol and deuterated chloroform solvent.

## 2.4. Instrumentation

**2.4.1.  $^1\text{H-NMR}$  Measurement.** The  $^1\text{H-NMR}$  test was completed by using a German Bruker VANCE 400 MHz H-nuclear magnetic resonance apparatus at room temperature by TMS internal standard. The sample concentration was set at 4–5 mg/mL. To prepare the sample, 16–20 mg POM was dissolved in 1 mL of 1,1,1,3,3,3-hexafluoro-2-propanol (HFIP), then, 3 mL of deuterated chloroform was added to the solution.

**2.4.2. Infrared Measurement.** The structure of POM copolymers was characterized using NICOLET 380 FTIR infrared spectrometer. Sample powder is mixed with KBr and molded into the specimen.

**2.4.3. TG Measurement.** The thermal stability of polyoxymethylene was characterized by using a Q500 TGA (TA Co., US) under a nitrogen atmosphere. The temperature range was set from room temperature to 600°C, with a heating rate of 10°C/min. The atmosphere gas flow rate was 50 mL/min.

**2.4.4. DSC Measurement.** The DSC test was characterized by using a Q2000 DSC instrument (TA Co., USA). The test has been carried out under a nitrogen atmosphere with a nitrogen flow rate of 50 mL/min. Specimens were heated from 40°C to 190°C, isothermal for 5 minutes, then cooled down

to room temperature. The heating/cooling rate was set at 10°C/min. Thermal history was removed before the tests.

**2.4.5. GPC Measurement.** The molecular weight was determined by using TRSEC MODEL302 (Viscotek Co., USA). The solvent was 1,1,1,3,3,3-hexafluoro-2-propanol (HFIP).

**2.5. Simulation.** In order to characterize the copolymerization ability of different second monomers with TOX, those comonomers were modeled by using Gaussian View software. The energy barrier of copolymerization was calculated by using Gaussian09 [29]. The progress of ring-opening copolymerization of TOX with the second monomer was studied according to density functional theory (DFT). The difficulty of the reaction was investigated by analyzing the reaction kinetics. The structure optimization and energy calculation of the reactants, transition states, and products were done under the b3lyp and 6-31G(d) basis sets method, and gd3bj dispersion correction was also put into consideration. To confirm the pole characteristics of the potential energy surface (all positive frequencies correspond to the stable state and the only imaginary frequency corresponds to the transition state), the calculation of the resonance frequency is also carried out at b3lyp/6-31G(d) methods. Finally, the intrinsic reaction coordinate (IRC) method was used to construct the reaction minimum energy path (MEP). In order to keep the accuracy of the simulation data, the zero-point

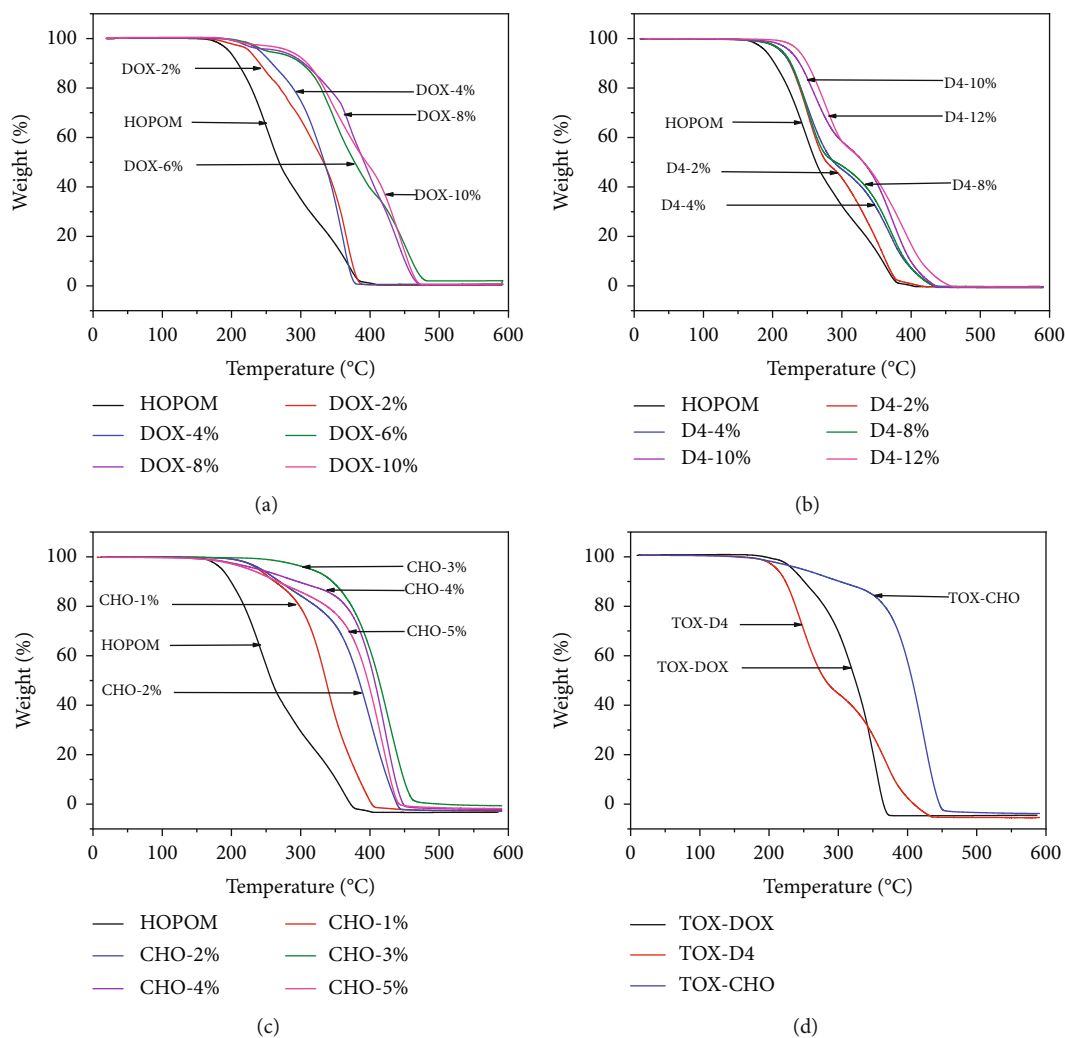


FIGURE 3: TGA curves of the copolymer. (a) Changes in the dosage of DOX. (b) Changes in the dosage of D4. (c) Changes in the dosage of CHO. (d) Comparison of the second monomer (4 mol%).

vibration correction was applied to all energy calculations, according to Heisenberg's uncertainty principle.

### 3. Results and Discussion

**3.1. Cationic Copolymerization of TOX and the Second Monomer.** Take the second monomer DOX as an example, the productivities and molecular weights of the synthesized copolymers with different initiator dosages are listed in Table 2.  $M_n$  in Table 2 is determined by GPC, as shown in Section 2.4.5. It can be found that when the concentration of boron trifluoride is up to 20 ppm, the polymerization cannot be initiated. In industrial production, the concentration of boron trifluoride initiator is usually more than 50 ppm to ensure a high level of productivity. The necessary concentration of phosphotungstic acid initiator to synthesize POM is much lower. 6 ppm is enough to initiate polymerization. What is more, the molecular weight of the copolymer decreases with the increase of initiator dosage, which benefits the posttreatment of POM, helping with the improvement of thermal stability.

However, the polymerization rate positively correlated to initiator concentration. To balance the polymerization rate and molecular weight, a 10 ppm initiator concentration was chosen. At this concentration, the copolymerization of TOX and 1% of CHO exhibits a very short induction period (less than 20 s), and the solution cured quickly (less than 2 min). The induction period extended with the increase of the dosage of the second monomer. The molar ratio of the second monomers fed to the system and synthesized into the copolymer are listed in Table 3, respectively. When the dosage of the second monomer is 2%, the synthesized CHO in the copolymer structure is 0.27 mol% higher than that of DOX. Similarly, at a 4% second monomer feeding level, CHO is still the largest second monomer synthesized into the copolymer.

#### 3.2. Structural Characterization

**3.2.1. FTIR Analysis.** The FTIR spectra of copolymers prepared by TOX with second monomers have been demonstrated in Figure 1, respectively. In the case of a copolymer

TABLE 4: TG and DSC results of the copolymer.

Serial number	Sample	Thermal decomposition temperature <sup>c)</sup> (°C)	Melting temperature <sup>d)</sup> (°C)	Melting enthalpy <sup>d)</sup> (J/g)	Crystallinity (%)
	HOPOM	209.05	172.15	124.3	49.85
	p(TOX-co-DOX)				
1	p(TOX <sub>98</sub> -co-DOX <sub>2</sub> )	306.54	168.79	123.1	49.37
2	p(TOX <sub>96</sub> -co-DOX <sub>4</sub> )	308.35	166.99	118.6	47.56
3	p(TOX <sub>94</sub> -co-DOX <sub>6</sub> )	309.17	165.90	116.7	46.80
4	p(TOX <sub>92</sub> -co-DOX <sub>8</sub> )	338.07	164.88	107.8	43.23
5	p(TOX <sub>90</sub> -co-DOX <sub>10</sub> )	358.67	163.37	103.2	41.39
	p(TOX-co-D4)				
6	p(TOX <sub>98</sub> -co-D4 <sub>2</sub> )	226.40	172.12	129.7	52.01
7	p(TOX <sub>96</sub> -co-D4 <sub>4</sub> )	229.37	172.23	132.5	53.02
8	p(TOX <sub>92</sub> -co-D4 <sub>8</sub> )	234.21	173.33	119.8	48.04
9	p(TOX <sub>90</sub> -co-D4 <sub>10</sub> )	236.81	173.03	121.9	48.89
10	p(TOX <sub>88</sub> -co-D4 <sub>12</sub> )	249.50	172.17	121.1	48.56
	p(TOX-co-CHO)				
11	p(TOX <sub>99</sub> -co-CHO <sub>1</sub> )	304.52	168.09	129.9	52.09
12	p(TOX <sub>98</sub> -co-CHO <sub>2</sub> )	349.92	166.60	131.8	52.86
13	p(TOX <sub>97</sub> -co-CHO <sub>3</sub> )	383.03	155.65	123.7	49.60
14	p(TOX <sub>96</sub> -co-CHO <sub>4</sub> )	381.31	154.85	104.8	42.01
15	p(TOX <sub>95</sub> -co-CHO <sub>5</sub> )	372.72	140.89	56.7	22.72

<sup>c)</sup>Data from TGA results. <sup>d)</sup>Data from DSC results.

of TOX and DOX, the characteristic peaks of acetal structures around  $894\text{ cm}^{-1}$ - $934\text{ cm}^{-1}$  and  $1095\text{ cm}^{-1}$ - $1283\text{ cm}^{-1}$  can be observed. The observed peak at  $1385\text{ cm}^{-1}$  belongs to the bending vibration of  $\text{CH}_2$  and the stretching vibration of the C-C bond, which confirmed the DOX was synthesized into the backbone of POM. The results agree with Khadidja Beloufa's report [12]. The absorption peak of Si-O-Si of polydimethylsiloxane is located at  $1027$ - $1088\text{ cm}^{-1}$ , which can be found in the plot of TOX + D4. Si-O-C has a strong absorption peak at  $1000$ - $1100\text{ cm}^{-1}$ . Thus, the copolymer synthesized by TOX and D4 has strong absorption broadband at  $1000$ - $1140\text{ cm}^{-1}$  [19], which proves that dimethylsiloxane-(OSi(CH<sub>2</sub>)<sub>2</sub>)-structures have been successfully synthesized into the backbone. In the curve of TOX and CHO copolymer, the out-of-plane vibrational peak of CH at  $894\text{ cm}^{-1}$  is strengthened [30], which proves that CHO structure exists in the polymer.

**3.2.2. <sup>1</sup>H-NMR Analysis.** The <sup>1</sup>H-NMR spectra of the copolymer are shown in Figure 2. The peaks at 3.54 ppm and 4.38 ppm represent HFIP. And the peak at 7.26 ppm represents to deuterated chloroform solvent. In all three plots of Figure 2, the methylene proton signal ( $H_a$ ) of the oxymethylene unit is observed at 4.89 ppm. The presence of the signal peak at 3.75 ppm in Figure 2(a) represents methylene protons in between two oxymethylene units ( $H_b$ ), indicating the comonomer units have entered the oxymethylene chain successfully [28]. In Figure 2(b), the proton peak ( $H_c$ ) of -OSi(CH<sub>2</sub>)<sub>2</sub> is observed at 0.12 ppm [31]. The peak at 2.23 ppm is the peak of the methylene proton attached to the siloxane (see Supporting Information, Figure S1). In

Figure 2(c), the proton peak of methylene groups (cyclohexane CH<sub>2</sub>) is between 1.0- 2.0 ppm. Prominent proton peaks ( $H_j$  at 1.40 ppm and  $H_k$  at 1.28 ppm) have been marked in the figure. The proton peak of methine groups (CH<sub>2</sub>-CHO) ( $H_i$ ) locates at 3.2-3.6 ppm [32], which partially overlaps with the HFIP solvent peak.

Through the characterization of IR and <sup>1</sup>H-NMR, it is proved that the second monomers have successfully synthesized into the polymer. To further characterize the copolymerization ability of different second monomers with TOX, the <sup>1</sup>H-NMR spectrum was detailedly analyzed. The peak integral areas of the <sup>1</sup>H-NMR spectrum correlated to the number of each type of protons. Thus, the mole ratio of each monomer in the polymer chain can be calculated through the following [28]. The calculation results are shown in Table 1.

$$\text{DOX : mol(\%)} = \frac{I_{Hb}/4}{(I_{Ha}/6) + (I_{Hb}/4)} \times 100, \quad (1)$$

$$\text{D4 : mol(\%)} = \frac{I_{Hc}/24}{(I_{Ha}/6) + (I_{Hc}/24)} \times 100, \quad (2)$$

$$\text{CHO : mol(\%)} = \frac{I_{Hj}/2}{(I_{Ha}/6) + (I_{Hj}/2)} \times 100. \quad (3)$$

Among them, equations (1)–(3) correspond to the respective peaks in Figures 3(a)–3(c).

For each comonomer, with the increase of the feeding mole fraction, the proportion of the second monomer in the final product increases. However, in comparison to



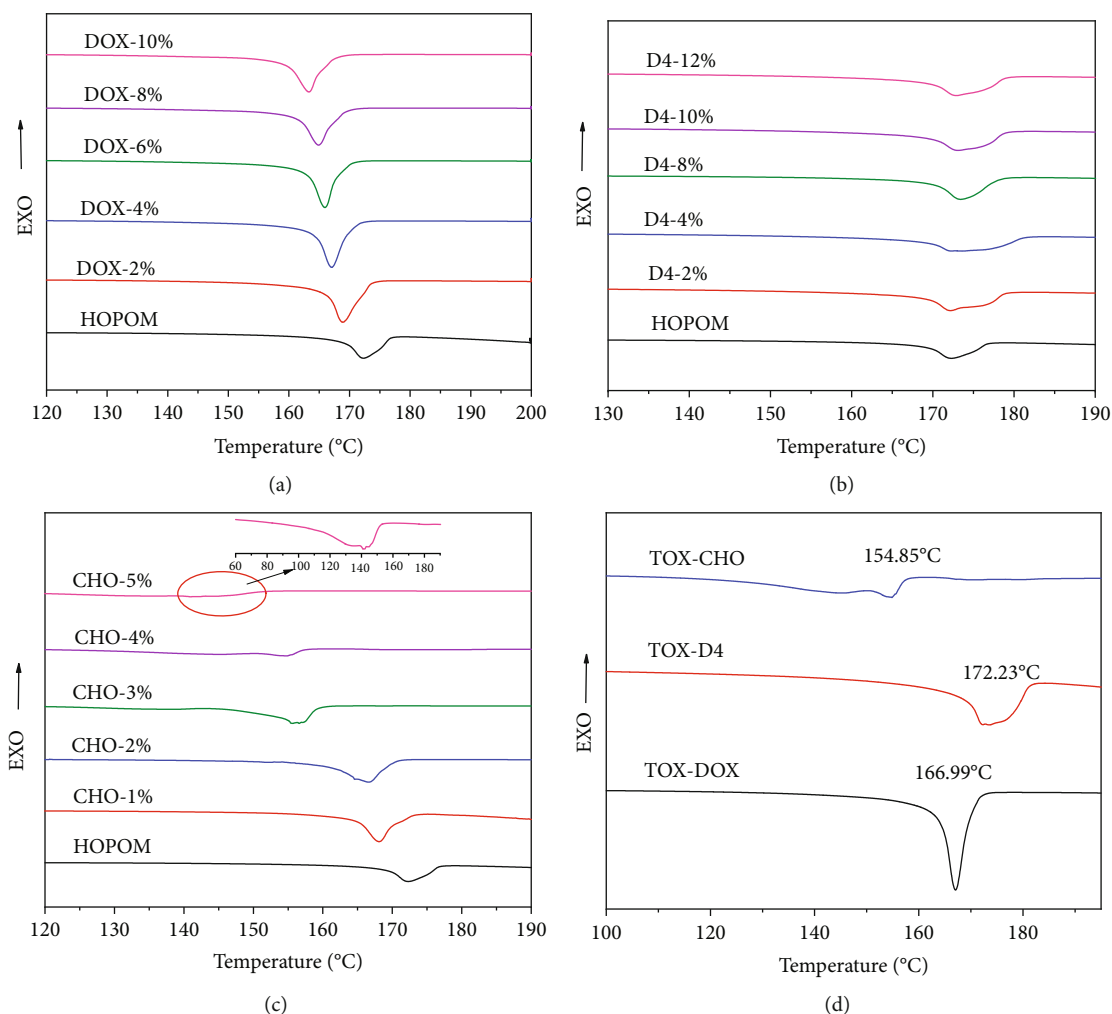
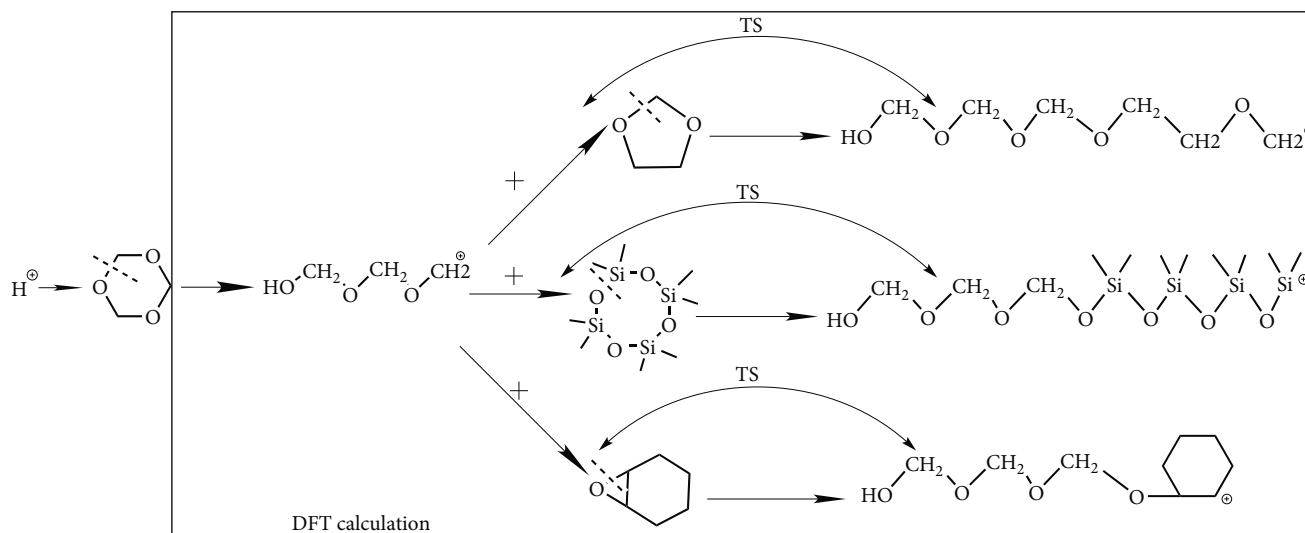


FIGURE 4: DSC curve of the copolymer. (a) Changes in the dosage of DOX. (b) Changes in the dosage of D4. (c) Changes in the dosage of CHO. (d) Comparison of the second monomers (4 mol%).

p(TOX-co-DOX) and p(TOX-co-CHO), the mole fraction of D4 is much smaller in the p(TOX-co-D4), indicating that D4 is not easy to participate in the copolymerization with TOX. When the feeding dosage of the second monomers is the same, the proportion of CHO units is the highest among those three comonomers. For example, when the feeding second monomer is 4%, the mole fraction of CHO, DOX, and D4 in the copolymer is 2.14%, 1.60%, and 0.31%, respectively. It shows that CHO as the second monomer is the easiest to participate in the copolymerization reaction.

**3.3. Thermal Stability.** In order to investigate the thermal stability of the synthesized copolymers, TGA tests were performed. Figure 3 presents the overlay of TGA curves of copolymer with different feeding ratios of TOX with second monomers. The thermal decomposition temperatures of each curve are shown in Table 4. All copolymers demonstrate better thermal stability than homo-polyoxymethylene (HOPOM). For example, the initial decomposition temperature of the p(TOX<sub>90</sub>-co-DOX<sub>10</sub>) is 358.67°C, while that of HOPOM is 209.05°C. The decomposition temperature has increased by 96°C. It shows that the introduction of DOX

to the copolymer dramatically enhanced the thermal stability of the copolymer. From the TGA curves in Figure 3(a), it can be found the starting decomposition temperature is positively related to the mole percentage of DOX in the copolymer. Two decomposition stages are observed in the TGA curves of p(TOX-co-D4) in Figure 3(b). In the first stage, the decomposition rate is high. It is believed the first stage of the decomposition takes place at the TOX-rich segments. In the second stage, the decomposition rate slows down, related to the chains with D4 units. With more D4 synthesized into the copolymer, the weight loss rate with temperature slowed down. The related degradation mechanism was drawn in the following chapter. For example, the weight loss of p(TOX<sub>98</sub>-co-D4<sub>2</sub>) is about 52% at the first stage. About 40% weight loss is observed for p(TOX<sub>90</sub>-co-D4<sub>10</sub>) at the first stage. And the largest thermal decomposition temperature of p(TOX-co-D4) is observed at 249.50°C. In Figure 3(c), it can be found the thermal stability of p(TOX<sub>97</sub>-co-CHO<sub>3</sub>) was the best among those three copolymers. The initial decomposition temperature reached 383.03°C. When the fraction of CHO was set at 3%, the copolymer achieved the best thermal stability. When three



SCHEME 2: The section of the DFT calculation of copolymerization of the second monomer with TOX.

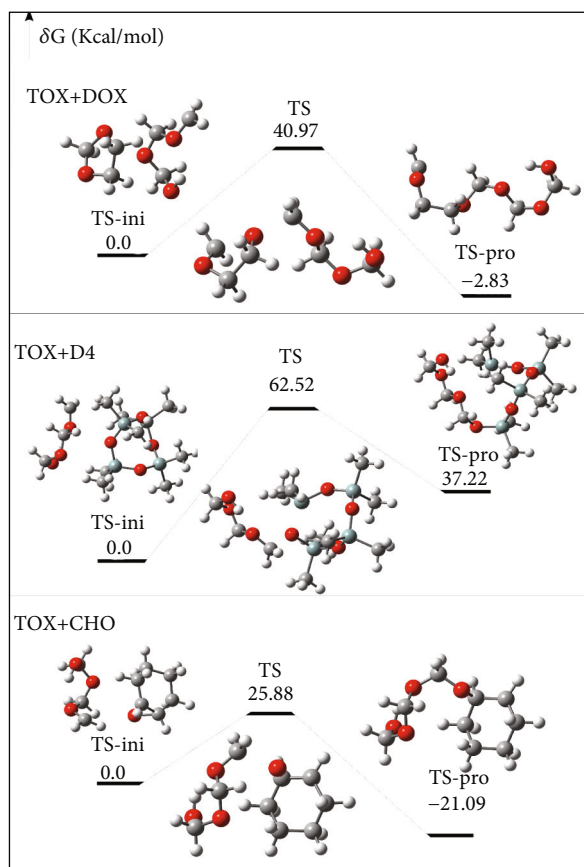
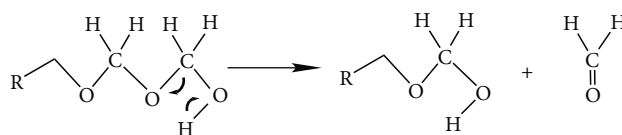


FIGURE 5: Energy barrier diagram of copolymerization of the second monomer with TOX.

second monomers are evaluated at the same feeding dosage (2% and 4%), the thermal stability beneficial ability can be ordered from high to low: CHO > DOX > D4.

**3.4. DSC Analysis.** Thermal properties of the copolymer were investigated via DSC and compared with that of HOPOM.



SCHEME 3: The depolymerization mechanism of HOPOM.

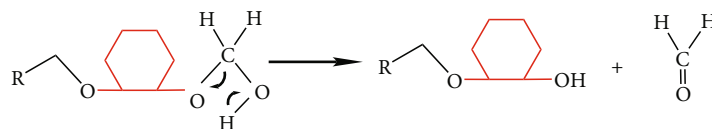
The results are shown in Figure 4. The melting peak of the polymers can be observed at all curves. The melting temperature and melting enthalpy of each copolymer were calculated. The crystallinity of the specimens was calculated by using equation (4). Results are shown in Table 4.

$$\text{Crystallinity } X_C(\%) = \left( \frac{\Delta H}{\Delta H^0} \right) \times 100, \quad (4)$$

where  $\Delta H$  represents the melting enthalpy of the sample, and  $\Delta H^0$  represents the melting enthalpy of 100% crystalline POM, which is reported as 249.36 J/g [28].

The crystallization comes from the regularity of the polymer units. In general, melting temperatures and the crystallinity of the copolymers decrease with the increase of the second monomer content, for second monomers interrupted the regularity of homo POM structures. It can be seen from Figure 4(a) that with the increase of DOX proportion, the melting temperature and melting enthalpy both reduced. The same phenomenon goes for D4 and CHO co-monomers. The copolymer of p(TOX-co-D4) in Figure 4(b) shows that with the increase in D4 feeding dosage, the melting temperature is close to HOPOM but the changing trend is not obvious. This is because only a small amount of D4 is involved in copolymerization. In Figure 4(c), the fraction of CHO has an obvious effect on the melting temperature of POM. With the increase of the feeding dosage of CHO, the melting temperature decreases significantly. The melting temperature dropping degree is larger than that of DOX. The reason is the molecular volume





SCHEME 4: The depolymerization mechanism of the copolymer in the presence of CHO.

of CHO is larger than that of DOX. It has a more serious influence on the crystallization of the polymer. This situation can be observed obviously in Figure 4(d).

**3.5. Simulation Results.** The copolymerization ability of different second monomers with TOX was simulated, based on the above experimental results. The section of the DFT calculation is listed in Scheme 2. IRC method was used to construct the reaction minimum energy path (MEP). It can be verified that the transition state structure is correct (see Supporting Information, Figure S2). For the coordinates of the reactants, transition states and products are listed in Supporting Information. The energy barrier diagram was drawn in Figure 5.

The activation energies of the copolymerization of DOX, D4, and CHO with TOX are 43.41 kcal/mol, 65.26 kcal/mol, and 27.51 kcal/mol, respectively. Thus, the copolymerization ability of the second monomer with TOX in descending order is CHO > DOX > D4. According to the energy difference between reactants and products, CHO is the most likely to form copolymers with TOX among the three comonomers. Also, p(TOX-co-CHO) performed better thermal stability than that of other copolymers, which matches the experimental results. The copolymerization ability of D4 with TOX is the weakest. The comonomer is difficult to participate in the copolymerization with TOX. It agrees with the synthesized results.

**3.6. Depolymerization Mechanism.** Experimental results show that all copolymers demonstrate better thermal stability than homo-polyoxymethylene (HOPOM). The reason is that introduction of the second monomer unit into POM chains prevented the depolymerization process. When the unstable hemiacetal is heated, the formaldehyde released continuously, and a new hemiacetal terminal group will be generated, which is caused by the active hydrogen of the terminal hydroxyl. The depolymerization progress of POM began from the unstable hydroxyl groups at the chain end and then proceeds sequentially along the backbone chain, resulting in the catastrophic decomposition of the POM chain (Scheme 3) [27, 33].

The introduction of comonomer units into the POM backbone avoids the complete unzipping of the macromolecular chain since the depolymerization is stopped at comonomer units [14, 34–36]. The synthesized comonomer structure broke up the alternating C–O bonds, preventing the formation of the new hemiacetal terminal group. Take CHO comonomer as an example, depolymerization stopped where a six-membered ring existed because it formed stable end groups at this location. Thus, the thermal stability of

POM can be improved. The mechanism in the presence of CHO is as follows (Scheme 4) [28, 37].

## 4. Conclusion

In this paper, the cationic copolymerization of the second monomers DOX, D4, and CHO with TOX by bulk polymerization was studied by a combination of experiments and DFT calculation. The copolymerization of POM improved thermal stability. The order of the second monomer benefit to the thermal stability of POM from high to low was CHO > DOX > D4. Since adding the second monomer structural unit into the backbone destroys the structural regularity, the melting temperature, and crystallinity of the copolymer decrease. According to DFT calculation results, the copolymerization ability of the second monomer with TOX is in descending order: CHO > DOX > D4, which agrees with the experimental results. CHO as the second monomer was screened out more easily to participate in the copolymerization reaction, and the copolymerized product showed the best thermal stability among the three comonomers.

## Data Availability

The data used to support the findings of this study are included within the article. Further data or information is available from the corresponding author upon request.

## Conflicts of Interest

The authors declare no conflicts of interest.

## Authors' Contributions

Yushun Jin and Yibo Wu contributed equally to this work.

## Acknowledgments

This research was funded by the National Natural Science Foundation of China (no. 52073033), Beijing excellent talents training fund (no. Z2019-042), and Kailuan Group project.

## Supplementary Materials

Supplementary Materials Figures showing the  $^1\text{H-NMR}$  spectra of the copolymer of TOX with D4 and the IRC calculation of the copolymer of TOX with the second monomers. In addition, information about the coordinates of the reactants, transition states, and products in the DFT calculation. (*Supplementary Materials*)

## References

- [1] Y. Gao, S. Sun, Y. He, X. Wang, and D. Wu, "Effect of poly(ethylene oxide) on tribological performance and impact fracture behavior of polyoxymethylene/polytetrafluoroethylene fiber composites," *Composites Part B Engineering*, vol. 42, no. 7, pp. 1945–1955, 2011.
- [2] F. Wang, J. K. Wu, H. S. Xia, and Q. Wang, "Polyoxymethylene/carbon nanotubes composites prepared by solid state mechanochemical approach," *Plastics Rubber & Composites*, vol. 36, no. 7-8, pp. 297–303, 2007.
- [3] R. L. Smorada, "Encyclopedia of polymer science and engineering," *New York*, vol. 10, pp. 227–253, 1987.
- [4] Y. J. Mergler, R. P. Schaake, and A. Veld, "Material transfer of POM in sliding contact," *Wear*, vol. 256, no. 3-4, pp. 294–301, 2004.
- [5] S. M. Lebedev, O. S. Gefle, E. T. Amitov, D. V. Zhuravlev, and D. Y. Berchuk, "Thermophysical, rheological and morphological properties of polyoxymethylene polymer composite for additive technologies," *Russian Physics Journal*, vol. 61, no. 6, pp. 1029–1033, 2018.
- [6] V. W. Kern and H. Cherdron, "Der abbau von polyoxymethylenen. Poloxymethylene. 14. Mitteilung," *Macromolecular Chemistry & Physics*, vol. 40, no. 1, pp. 101–117, 1960.
- [7] A. Aronson, K. Tartakovsky, R. Falkovich et al., "Failure analysis of aging in polyoxymethylene fuel valves using fractography and thermal-FTIR analysis," *Engineering Failure Analysis*, vol. 79, pp. 988–998, 2017.
- [8] K. Pielichowska, K. Król, and T. M. Majka, "Polyoxymethylene-copolymer based composites with PEG-grafted hydroxyapatite with improved thermal stability," *Thermochimica Acta*, vol. 633, pp. 98–107, 2016.
- [9] S. H. Jenkins and P. J. Oliver, "Preparation of Formaldehyde Polymers with Improved Thermal Stability," US Patent 2964500, 1960.
- [10] J. Masamoto, K. Matsuzaki, T. Iwaisako, K. Yoshida, K. Kagawa, and H. Nagahara, "Development of a new advanced process for manufacturing polyacetal resins. Part III. End-capping during polymerization for manufacturing acetal homopolymer and copolymer," *Journal of Applied Polymer Science*, vol. 50, no. 8, pp. 1317–1329, 1993.
- [11] K. Król-Morkisz, E. Karaś, T. M. Majka, K. Pielichowski, and K. Pielichowska, "Thermal stabilization of polyoxymethylene by PEG-functionalized hydroxyapatite: examining the effects of reduced formaldehyde release and enhanced bioactivity," *Advances in Polymer Technology*, vol. 2019, Article ID 9728637, 17 pages, 2019.
- [12] K. Beloufa, N. Sahli, and M. Belbachir, "Synthesis of copolymer from 1,3,5-trioxane and 1,3-dioxolane catalyzed by magh-nite-H+," *Journal of Applied Polymer Science*, vol. 115, no. 5, pp. 2820–2827, 2010.
- [13] N. Vila Ramirez, M. Sanchez-Soto, S. Illescas, and A. Gordillo, "Thermal degradation of polyoxymethylene evaluated with FTIR and spectrophotometry," *Polymer-Plastics Technology and Engineering*, vol. 48, no. 4, pp. 470–477, 2009.
- [14] V. Archodoulaki, S. Luftl, and S. Seidler, "Thermal degradation behaviour of poly(oxymethylene): 1. Degradation and stabilizer consumption," *Polymer Degradation and Stability*, vol. 86, no. 1, pp. 75–83, 2004.
- [15] K. Matsuzaki, T. Hata, T. Sone, and J. Masamoto, "New Polyacetal process from formaldehyde polymerization in the presence of a chain transfer agent," *Bulletin of the Chemical Society of Japan*, vol. 67, no. 9, pp. 2560–2566, 1994.
- [16] S. Kucukyavuz and T. Nugay, "Radiation induced copolymerization of trioxane and maleic anhydride," *European Polymer Journal*, vol. 26, no. 4, pp. 485–487, 1990.
- [17] I. Yukio and Y. Masami, "Polyacetal resin composition," US Patent 4596847 A, 1988.
- [18] Y. Mu, M. Jia, W. Jiang, and X. Wan, "A novel branched polyoxymethylene synthesized by cationic copolymerization of 1,3,5-trioxane with 3-(alkoxymethyl)-3-ethyloxetane," *Macromolecular Chemistry & Physics*, vol. 214, no. 23, pp. 2752–2760, 2013.
- [19] M. Rodríguez-Baeza and M. Zapata, "Synthesis and characterization of copolymers obtained from 1,3,5-trioxane and octamethylcyclotetrasiloxane by triflic acid initiator," *Polymer Bulletin*, vol. 36, no. 2, pp. 173–180, 1996.
- [20] L. Guo, X. Xu, Y. Zhang, and Z. Zhang, "Effect of functionalized nanosilica on properties of polyoxymethylene-matrix nanocomposites," *Polymer Composites*, vol. 35, no. 1, pp. 127–136, 2014.
- [21] Y. Hu, Z. Xin, and Y. Lin, "Synergistic thermal stabilization effect of polyamide/melamine on polyoxymethylene," *Journal of Applied Polymer Science*, vol. 97, no. 6, pp. 2387–2391, 2005.
- [22] L. Gan and L. Ye, "The thermal stabilization effect of biphenol monoacrylate on polyoxymethylene," *Journal of Thermoplastic Composite Materials*, vol. 23, no. 4, pp. 543–559, 2010.
- [23] S. Penczek, J. Fejgin, P. Kubisa, K. Matyjaszewski, and M. Tomaszewicz, "New highly efficient initiators for the copolymerization of 1, 3-dioxolane with 1, 3, 5-trioxane based on the derivatives of trifluoromethanesulfonic acid [J]," *Die Makromolekulare Chemie*, vol. 172, no. 1, pp. 243–247, 1973.
- [24] L. Demejo, W. J. Macknight, and O. Vogl, "Poly(alkylene oxide) ionomers: 1. Copolymerization of trioxane by gas phase mixing of comonomers and initiator," *Polymer*, vol. 19, no. 8, pp. 956–962, 1978.
- [25] K. Sharavanan, E. Ortega, M. Moreau et al., "Cationic copolymerization of 1,3,5-trioxane with 1,3-dioxepane: a comprehensive approach to the polyacetal process," *Macromolecules*, vol. 42, no. 22, pp. 8702–8710, 2009.
- [26] N. Yamasaki, J. Masamoto, and K. Kanaori, "NMR spectra of cyclic formals formed during the early stage of the copolymerization of trioxane and ethylene oxide," *Applied Spectroscopy*, vol. 54, no. 7, pp. 1069–1074, 2000.
- [27] H. Jashni, S. Ahmadi, H. Arabi, and S. Dolatshah, "Thermal stabilization of polyoxymethylene by copolymerization and modified phenolic stabilizer: examining the effects of catalyst, retardant, and stabilizer," *Polymer-Plastics Technology and Materials*, vol. 60, no. 11, pp. 1203–1219, 2021.
- [28] M. A. Hajihashemi, S. Ahmadi, and H. Arabi, "Bulk copolymerization of 1, 3, 5-trioxane and 1, 3-dioxolane in presence of phosphotungstic acid catalyst and tetrahydrofuran as retarder: crystallinity and thermal properties," *Designed Monomers & Polymers*, vol. 19, no. 4, pp. 361–368, 2016.
- [29] M. J. E. A. Frisch, G. W. Trucks, H. B. Schlegel et al., *Gaussian 09, Revision D.01*, Gaussian, Inc., Wallingford CT, 2009.
- [30] A. Ahmed, A. O. Z. Abdullah, and S. Abdurrahman, "Keggin-type heteropolyacid for ring-opening polymerization of cyclohexene oxide: molecular weight control," *International Journal of Polymer Science*, vol. 2015, Article ID 826512, 6 pages, 2015.

- [31] D. E. Kherroub, M. Belbachir, S. Lamouri, and K. Chikh, "Cationic ring opening polymerization of octamethylcyclotrisiloxane using a cost-effective solid acid catalyst (maghnite-H<sup>+</sup>)," *Iranian Journal of Science and Technology*, vol. 43, no. 1, pp. 75–83, 2019.
- [32] J. Ling, L. You, Y. Wang, and Z. Shen, "Ring-opening polymerization of cyclohexene oxide by recyclable scandium triflate in room temperature ionic liquid," *Journal of Applied Polymer Science*, vol. 124, no. 3, pp. 2537–2540, 2012.
- [33] F. R. Stohler and K. Berger, "Stabilization of polyacetals," *Angewandte Makromolekulare Chemie*, vol. 176, no. 1, pp. 323–332, 1990.
- [34] S. Luftl, V. Archodoulaki, and S. Seidler, "Thermal-oxidative induced degradation behaviour of polyoxymethylene (POM) copolymer detected by TGA/MS," *Polymer Degradation & Stability*, vol. 91, no. 3, pp. 464–471, 2006.
- [35] Y. Duan, H. Li, L. Ye, and X. Liu, "Study on the thermal degradation of polyoxymethylene by thermogravimetry–Fourier transform infrared spectroscopy (TG–FTIR)," *Journal of Applied Polymer Science*, vol. 99, no. 6, pp. 3085–3092, 2006.
- [36] F. Yang, H. Li, L. Cai, F. Lan, and M. Xiang, "Degradation and stabilization of co-POM," *Polymer-Plastics Technology and Engineering*, vol. 48, no. 5, pp. 530–534, 2009.
- [37] V.-M. Archodoulaki and S. Lüftl, "Thermal Properties and Flammability of Polyoxymethylene, Polyoxymethylene Handbook," in pp. 257–275, John Wiley & Sons, Inc., 2014.